Supplemental Information

Dey et al. 10.1073/pnas.1014872108

SI Methods

NMR Methods. The bacterial expression vector encoding residues 3 to 175 of *Saccharomyces cerevisiae* eIF2α was described previously (1). Isotopically labeled WT eIF2α, eIF2α–L50S, and eIF2α–I62G were obtained from 2-L cultures in minimal M9 media containing [U-98%] 1.0 g/L ^{15}N-ammonium chloride as the sole source of nitrogen, or [U-98%] 1.0 g/L ^{15}N-ammonium chloride and [U-99%] 2.0 g/L ^{13}C-glucose as nitrogen and carbon sources, respectively. All eIF2α proteins were purified as described previously (1) with the final size exclusion chromatography step using a buffer solution containing 20 mM sodium phosphate, pH = 7.0 and 350 mM Na_2SO_4, 10 mM DTT, 0.5 mM EDTA, and 0.5 mM benzamidine. Proteins were concentrated to 0.5–0.9 mM in 0.5 mL for NMR analysis, and 10% of D_2O was added to each sample for spectrometer field lock. Backbone assignments of all nonproline residues (except Lys162) of WT protein were derived from a suite of triple-resonance spectra (2) and a 3D ^{15}N-edited NOESY (3), recorded at 25 °C on a 500 MHz spectrometer (room temperature probe) using an ^{15}N/^{13}C-labeled sample. Assignments of two mutant proteins were obtained by direct transfer from the WT protein for the majority of residues; sets of HNCA, HNCO and HN(CA)CO experiments on ^{15}N/^{13}C-labeled samples were sufficient to derive assignments for the Ser51 loop and to confirm the accuracy of assignments over the entire sequence of mutant proteins. The TALOS+ software package was used to convert backbone chemical shifts to order parameter values using the random coil index approach (4, 5). A transverse relaxation optimized spectroscopy (TROSY) version of $\{^1H\} - {}^{15}N$ NOE experiment was recorded on ^{15}N-only labeled samples at 25 °C on an 800-MHz spectrometer (room temperature probe); 100 points were collected in the indirect dimension (2240-Hz spectral window), 24 transients per point; recycle delays were 9 s of recovery followed by 6 s of saturation of amide protons or 15 s of recovery (no saturation) in the reference spectrum. Spectra were processed and peak intensities measured using the nmrPipe software package (6).

1. Dar AC, Dever TE, Sicheri F (2005) Higher-order substrate recognition of eIF2α by the RNA-dependent protein kinase PKR. *Cell* 122:887–900.
2. Sattler M, Schleucher J, Griesinger C (1999) Heteronuclear multidimensional NMR experiments for the structure determination of proteins in solution employing pulsed field gradients. *Prog Nucl Mag Reson Spectrosc* 34:93–158.
3. Zhang O, Kay LE, Olivier JP, Forman-Kay JD (1994) Backbone ^{1}H and ^{15}N resonance assignments of the N-terminal SH3 domain of drk in folded and unfolded states using enhanced-sensitivity pulsed field gradient NMR techniques. *J Biomol NMR* 4:845–858.
4. Shen Y, Delaglio F, Cornilescu G, Bax A (2009) TALOS+: A hybrid method for predicting protein backbone torsion angles from NMR chemical shifts. *J Biomol NMR* 44:213–223.
5. Berjanskii MV, Wishart DS (2005) A simple method to predict protein flexibility using secondary chemical shifts. *J Am Chem Soc* 127:14970–14971.
6. Delaglio F, *et al.* (1995) NMRPipe: a multidimensional spectral processing system based on UNIX pipes. *J Biomol NMR* 6:277–293.

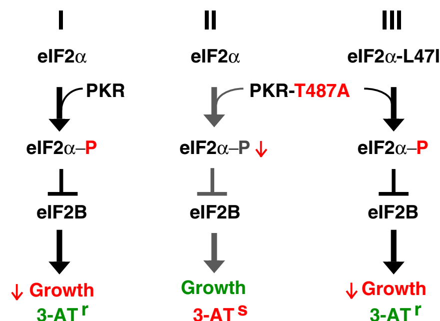

Fig. S1. Schematics of PKR growth phenotypes in yeast. (Scheme I) Phosphorylation of WT eIF2α by PKR results in eIF2B inhibition, poor yeast growth, and induction of *GCN4* expression conferring a 3-AT–resistant phenotype. (Scheme II) Impaired phosphorylation of eIF2α by PKR–T487A reverses the growth phenotypes. (Scheme III) The eIF2α–L47I mutation restores phosphorylation by PKR–T487A and the WT growth phenotypes.

Fig. S2. eIF2α Leu47 mutations and GCN2. (*A*) eIF2α–L47V and eIF2α–L47C mutations enhance PKR–T487A toxicity in yeast. Plasmids expressing PKR or PKR–T487A under control of a yeast *GAL–CYC1* hybrid promoter were introduced into yeast strains expressing the indicated eIF2α proteins. Transformants were grown to saturation, and 4 mL of serial dilutions (of $OD_{600} = 1.0, 0.1, 0.01$) were spotted on minimal SD and SGal medium and incubated 3 d at 30 °C. (*B*) eIF2α–L47I mutation restores *GCN4* translational control in yeast expressing the helix αG mutant GCN2–T924A. Yeast strains expressing the indicated WT and mutant versions of eIF2α were transformed with an empty vector or plasmids expressing GCN2 or GCN2–T924A under the control of its native promoter. Transformants were grown, serially diluted and spotted on SD and SD plus 3-AT (30 mM) medium supplemented with essential nutrients. Plates were incubated 3 d at 30 °C.

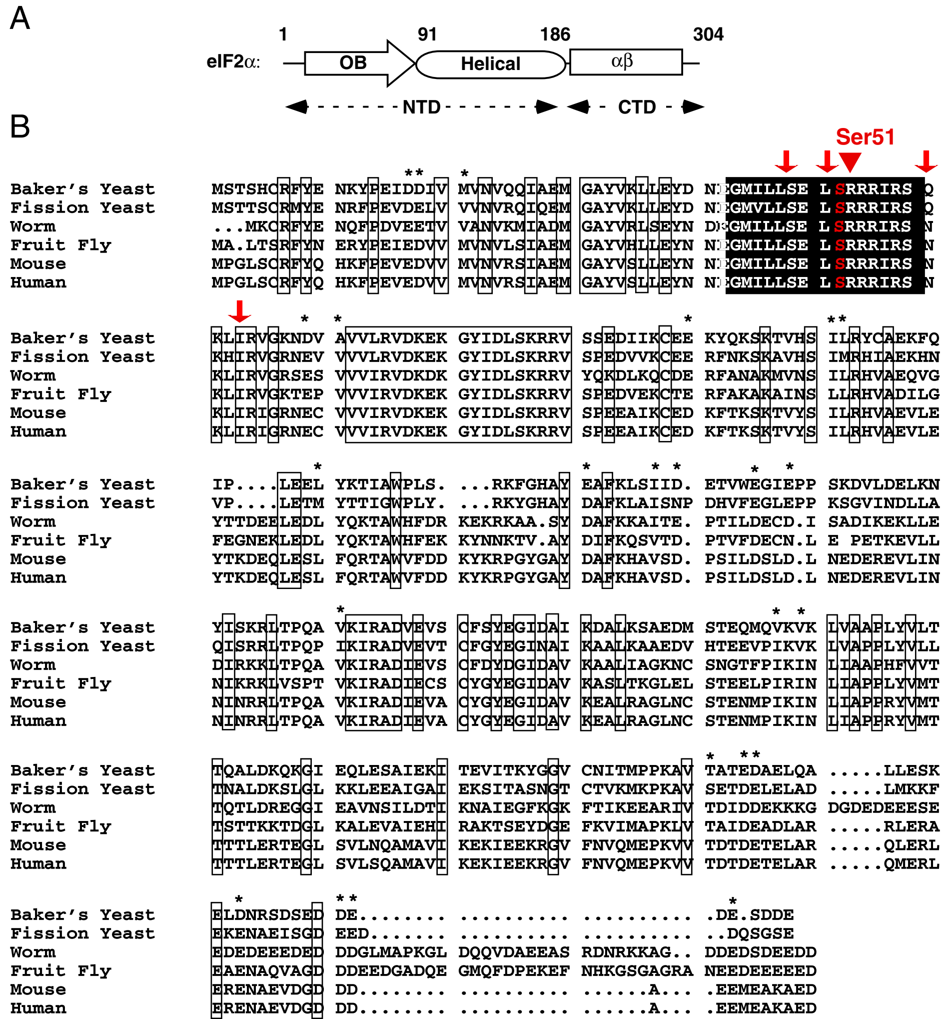

Fig. S3. Conservation of eIF2α primary and tertiary structures. (*A*) Schematic of eIF2α structure depicting the N-terminal domain (NTD) composed of an OB-fold and helical domain and the C-terminal domain (CTD) containing an αβ fold. (*B*) Multiple amino acid sequence alignment of eIF2α from *Saccharomyces cerevisiae* (baker's yeast); *Schizosaccharomyces pombe* (fission yeast), *Caenorhabditis elegans* (worm); *Drosophila melanogaster* (fly); *Mus musculus*; and *Homo sapiens* (human). Identical residues are boxed. Perfect sequence conservation flanking Ser51 (red) is shown in reverse type. Residues participating in the hydrophobic network surrounding Ser51 are marked by red arrows.

Fig. S4. eIF2α–L50S, –I58G and –I62G mutations restore Ser51 phosphorylation by PKR–T487D in vivo. (*A*, *C*, and *E*) Derivatives of yeast strain H2507 expressing the indicated eIF2α and PKR proteins were grown to saturation, and 4 mL of serial dilutions (of OD_{600} = 1.0, 0.1, 0.01) were spotted on SD or SGal medium and incubated 3 d at 30 °C. (*B*, *D*, and *F*) Immunoblot analysis of eIF2α phosphorylation in yeast expressing PKR or PKR–T487A. Yeast strains expressing the indicated eIF2α and PKR proteins were grown to exponential phase in SC-ura medium and then shifted to SGal-ura medium for 2 h to induce PKR expression. Whole cell extracts were prepared and total proteins were subjected to immunoblot analysis with phospho-specific antibodies against Ser51 in eIF2α (*Upper*). The membranes were then stripped and probed using polyclonal antiserum against yeast eIF2α (*Lower*).

Fig. S5. Chemical shift changes due to L50S and I62G mutations cluster to the Ser51 loop and adjacent protein regions. (*A* and *B*) Chemical shift changes for each backbone amide group, defined as $\Delta\delta = (\Delta\delta(^1\mathrm{H})^2 + (\Delta\delta(^{15}\mathrm{N})/5)^2)^{1/2}$ plotted versus residue number for L50S (*A*) and I62G (*B*) mutants. Spheres with indicated colors and radii are employed to map chemical shift changes onto the protein structure of eIF2α in *C*and *D*. (*C* and *D*) Perturbation of chemical shifts in L50S mutant (*C*) from *A* and I62G mutant (*D*) from *B* shown on the structure of eIF2α (1–175) (Protein Data Bank code 1Q46). Spheres are drawn at positions of backbone N atoms.

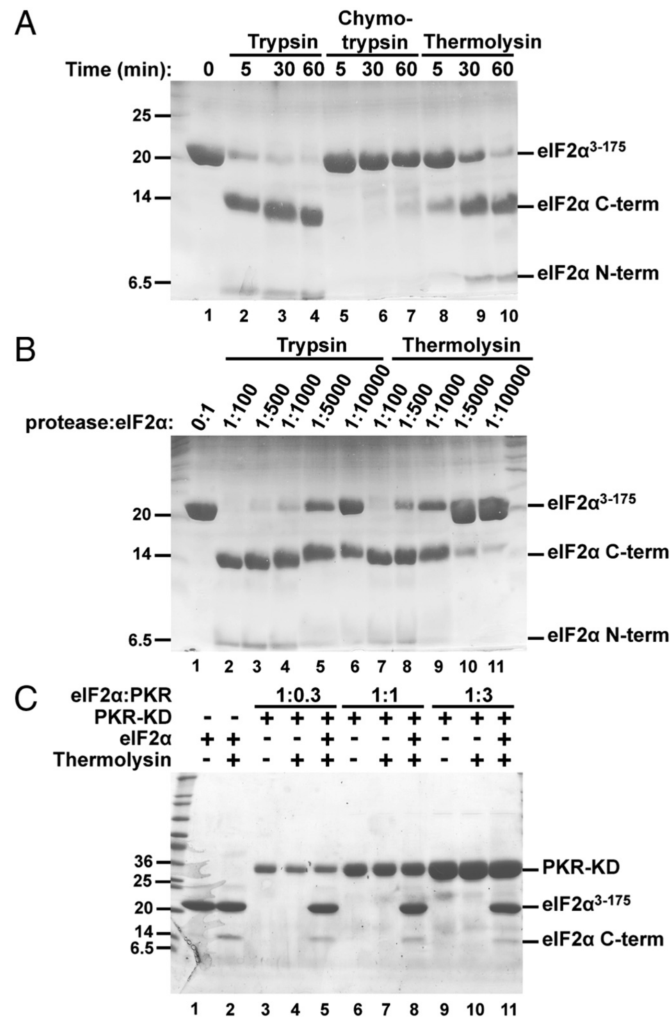

Fig. S6. Protease sensitivity of the Ser51 loop in eIF2α. (*A*) Purified yeast eIF2$\alpha^{3\text{–}175}$ was incubated for the indicated times with trypsin, chymotrypsin or thermolysin [1:1000 ratio (wt/wt)], as indicated. Protease reaction products were separated by SDS-PAGE and visualized by Coomassie Blue staining. The positions of intact eIF2$\alpha^{3\text{–}175}$, the eIF2α C-terminal cleavage product (starting at Leu61), and the eIF2α N-terminal cleavage product are indicated. (*B*) Purified yeast eIF2$\alpha^{3\text{–}175}$ was incubated for 30 min with the indicated ratios (wt/wt) of trypsin or thermolysin. Protease reaction products were analyzed as described in *A*. (*C*) Purified yeast eIF2$\alpha^{3\text{–}175}$ was incubated for 30 min with thermolysin [1:3500 ratio (wt/wt)], and the indicated ratio (wt/wt) of purified PKR kinase domain (KD). Protease reaction products were analyzed as described in *A*.

Fig. S7. Mutation of eIF2α OB-fold docking residue Met44 impairs Ser51 phosphorylation. (*A*) eIF2α OB-fold domain residues Tyr32 (in strand β2), Met44 (strand β3), and Asp83 (strand β5) dock on helix αG in the C-terminal lobe of the PKR kinase domain. (*B*) In vitro kinase assay. (*Left*) Recombinant GST–eIF2α^{1-180} and its indicated derivatives were mixed with [γ-^{33}P]ATP and purified PKR. Reaction products were analyzed as described in Fig. 2*B*. (*Right*) Kinetic analysis of PKR phosphorylation of eIF2α and eIF2α–M44V. Recombinant GST–eIF2α^{1-180} and GST–eIF2α^{1-180}–M44V were phosphorylated by purified PKR, and the relative incorporation of phosphate into eIF2α was determined using a PhosphorImager. Results are expressed in arbitrary units and are representative of at least two independent experiments; *kcat* units are sec^{-1}.

Table S1. Yeast plasmids employed in this study

Plasmid	Description	Source
pC171	sc *LEU2 SUI2* (eIF2α)	(1)
p1098	sc *LEU2 SUI2-S51A*	(2)
pC2425	sc *LEU2 SUI2-L47I* in pC171	this study
pC2426	sc *LEU2 SUI2-L471,S51A* in pC171	this study
pC3120	sc *LEU2 SUI2-I58G* in pC171	this study
pC3121	sc *LEU2 SUI2-I58G,S51A* in pC171	this study
pC2428	sc *LEU2 SUI2-I62G* in pC171	this study
pC2431	sc *LEU2 SUI2-I62G,S51A* in pC171	this study
pC3122	sc *LEU2 SUI2-L50S* in pC171	this study
pC2429	sc *LEU2 SUI2-L50S,S51A* in pC171	this study
pC3123	sc *LEU2 SUI2-L50P* in pC171	this study
pC3124	sc *LEU2 SUI2-L50P,S51A* in pC171	this study
pC3125	sc *LEU2 SUI2-D83A* in pC171	this study
pC3126	sc *LEU2 SUI2-S85A* in pC171	this study
pC3127	sc *LEU2 SUI2-S85D* in pC171	this study
pC3128	sc *LEU2 SUI2-D83A,S85A* in pC171	this study
pC3129	sc *LEU2 SUI2-D83A,S85D* in pC171	this study
pC3137	sc *LEU2 SUI2-L47R* in pC171	this study
pC3138	sc *LEU2 SUI2-L47N* in pC171	this study
pC3139	sc *LEU2 SUI2-L47V* in pC171	this study
pC3140	sc *LEU2 SUI2-L47H* in pC171	this study
pC3141	sc *LEU2 SUI2-L47Y* in pC171	this study
pC3142	sc *LEU2 SUI2-L47S* in pC171	this study
pC3143	sc *LEU2 SUI2-L47C* in pC171	this study
pC3144	sc *LEU2 SUI2-L47T* in pC171	this study
pC3188	sc *LEU2 SUI2-D83E* in pC171	this study
pC3189	sc *LEU2 SUI2-L50S,D83E* in pC171	this study
pC1685	hc *URA3 GAL-CYC1-PKR* in pEMBLyex4	this study
p2828	hc *URA3 GAL-CYC1-PKR-K296R* in pEMBLyex4	this study
pC1694	hc *URA3 GAL-CYC1-PKR-T487A* in pEMBLyex4	this study
pC1696	hc *URA3 GAL-CYC1-PKR-T487D* in pEMBLyex4	this study
pC3153	hc *TRP1 GAL-CYC1-PKR-T487A* in p2444	this study
p2444	hc *TRP1* derivative of pEMBLyex4	G. Pavitt/(3)
p722	sc *URA3 GCN2*	(4)
pC3179	sc *URA3 GCN2-T924A*	this study

1 Dey M, et al. (2005) PKR and GCN2 kinases and guanine nucleotide exchange factor eukaryotic translation initiation factor 2B (eIF2B) recognize overlapping surfaces on eIF2α. *Mol Cell Biol* 25:3063–3075.

2 Dever TE, et al. (1992) Phosphorylation of initiation factor 2α by protein kinase GCN2 mediates gene-specific translational control of *GCN4* in yeast. *Cell* 68:585–596.

3 Ung TL, Cao C, Lu J, Ozato K, Dever TE (2001) Heterologous dimerization domains functionally substitute for the double-stranded RNA binding domains of the kinase PKR. *EMBO J* 20:3728–3737.

4 Wek RC, Ramirez M, Jackson BM, Hinnebusch AG (1990) Identification of positive-acting domains in GCN2 protein kinase required for translational activation of *GCN4* expression. *Mol Cell Biol* 10:2820–2831.

Table S2. Bacterial expression plasmids employed in this study

Plasmid	Description	Source
pC1638	GST–eIF2α in pGEX-6P-1	(1)
pC1613	GST–eIF2α–S51A	(1)
pC2566	GST–eIF2α–I58G	this study
pC2567	GST–eIF2α–I58G,S51A	this study
pC2568	GST–eIF2α–I62G	this study
pC2569	GST–eIF2α–I62G,S51A	this study
pC3177	GST–eIF2α–L50S	this study
pC3178	GST–eIF2α–L50S,S51A	this study
pC2966	GST–eIF2α–L50P	this study
pC2967	GST–eIF2α–L50P,S51A	this study
pC2978	GST–eIF2α–D83A	this study
pC2979	GST–eIF2α–S85A	this study
pC2980	GST–eIF2α–S85D	this study
pC2981	GST–eIF2α–D83A,S85A	this study
pC2982	GST–eIF2α–D83A,S85D	this study
pC3786	GST–eIF2α–L50P,S51A,S57A	this study

1 Dey M, et al. (2005) PKR and GCN2 kinases and guanine nucleotide exchange factor eukaryotic translation initiation factor 2B (eIF2B) recognize overlapping surfaces on eIF2α. *Mol Cell Biol* 25:3063–3075.